Use of filler wire for laser welding of Ti–6Al–4V

A. S. H. Kabir[1,2], X. Cao*[1], P. Wanjara[1], J. Cuddy[3], A. Birur[3] and M. Medraj[2]

Owing to the high specific strength and excellent corrosion resistance, Ti–6Al–4V has been widely applied in aerospace industries. In this study, the welding performance of 3·2 and 5·1 mm thick Ti–6Al–4V sheets was studied using a 4 kW continuous wave Nd:YAG laser. It is found that the use of filler wire, matching the parent metal composition, can bridge the joint gap and produce full penetrated welds up to a width of 0·6 mm without cracking. The laser welds were characterised in terms of the bead geometry, defects, microstructures and hardness. With increasing joint gap, the percent porosity area increased, reaching just over 1% of the fusion zone area at a gap width of 0·6 mm for the 3·2 and 5·1 mm thick sheets. The maximum underfill depth in the Ti–6Al–4V laser welds was about 5% or 7% of the sheet thickness for the 3·2 and 5·2 mm thick materials, respectively, meeting the AWS D17-1 specification. The microindentation hardness was maximum in the fusion zone and sharply decreased through the heat affected zone until reaching the base metal value.

En raison de sa résistance spécifique élevée et de son excellente résistance à la corrosion, le Ti–6Al–4V est largement utilisé dans l'industrie aérospatiale. Dans cette étude, on a étudié le rendement de soudage de tôles de Ti–6Al–4V de 3·2 et 5·1 mm d'épaisseur en utilisant un laser Nd:YAG de 4 kW à onde continue. On constate que l'utilisation de fil d'apport, correspondant à la composition du métal parent, peut combler l'espace du joint et produire des soudures à pénétration complète sans fissures jusqu'à une largeur de 0·6 mm. On a caractérisé les soudures au laser en termes de la géométrie des cordons, des défauts, des microstructures et de la dureté. Avec l'augmentation de l'espace du joint, le pourcentage de porosité augmentait, atteignant un peu plus de 1% de la superficie de la zone de dilution avec une largeur de joint de 0·6 mm pour les tôles de 3·2 et 5·1 mm d'épaisseur. La profondeur maximale du caniveau dans les soudures au laser de Ti–6Al–4V était respectivement d'environ 5% ou 7% de l'épaisseur de la tôle pour les matériaux de 3·2 et 5·2 mm d'épaisseur, satisfaisant ainsi la norme d'AWS D17-1. La dureté de la micro-indentation était maximale dans la zone de dilution tout en diminuant fortement dans la zone thermiquement affectée jusqu'à atteindre ultimement la valeur du métal de base.

Keywords: Laser welding, Filler addition, Ti alloys, Microstructure, Mechanical properties

This paper is part of a special issue on Advances in High Temperature Joining of Materials

Introduction

Light weighting of primary aircraft structures has resulted in the gradual, and ever increasing, transition from aluminium to composite materials. Nonetheless, the regions of stress concentration in the composite materials need local reinforcement with metallic structures. Of the various possibilities, titanium alloys offer the highest electrochemical compatibility, with a concomitant high strength to weight ratio,[1] but their high raw material cost and relatively poor machinability and formability are strong motivators to introduce emerging manufacturing technologies that allow a reduction in the buy to fly ratio (i.e. minimised scrap). Hence, the development of cost efficient joining technologies has become an indispensable challenge for design and near net shape processing of titanium alloy structures.[2] Arc welding including plasma has been the traditional joining process widely used for titanium alloys.

[1]Aerospace Manufacturing Technology Center, Institute of Aerospace Research, National Research Council Canada, 5145 Decelles Avenue, Montréal, Qué. H3T 2B2, Canada
[2]Department of Mechanical and Industrial Engineering, Concordia University, 1455 De Maisonneuve Blvd. West, Montréal, Qué. H3G 1M8, Canada
[3]Standard Aero Limited, 33 Allen Dyne Road, Winnipeg, Man. R3H 1A1, Canada

*Corresponding author, email Xinjin.Cao@cnrc-nrc.gc.ca

Published by Maney on behalf of the Institute
Received 26 October 2011; accepted 7 March 2012
DOI 10.1179/1879139512Y.0000000016

However, the high reactivity of titanium with atmospheric gases at high temperatures above 400°C, especially in the liquid state, has led to the use of high vacuum electron beam welding process, particularly for the aerospace industry.[3] To this end, laser welding shows high potential for joining titanium alloys due to its high energy density that allows low heat input (laser power/welding speed) and fast welding speed. Laser welded assemblies benefit from high aspect ratio welds (penetration depth/bead width ratio) that exhibit a narrow heat affected zone (HAZ), low distortion and a refined prior beta grain size.[1,3,4]

A shortfall of autogenous laser welding is the precise fit-up requirement for the joint geometry that transpires from the small laser beam size.[5] The fit-up tolerance (joint gap) can be increased through the use of a filler material,[5,6] which can also compensate for metal loss due to vaporisation.[1,7] Though the filler metal composition is usually matched to the grade of the titanium alloy being welded,[8] the use of an unalloyed filler metal can improve the joint ductility of Ti–6Al–4V by reducing the extent of the (martensitic) transformation that occurs during rapid solidification after laser welding.[9] Filler material forms include wire, strip or powder, of which the most practical for high production capacity and low contaminant pick-up in titanium alloys is the application of a continuous wire feed system.[5] As compared to autogenous laser welding, the utilisation of wire feeding requires an increase in the laser power or a decrease in the welding speed[7] for a given penetration depth, inevitably due to several factors: (1) beam energy allocation to melt the wire; (2) energy loss from reflection off the wire; and (3) energy loss through the joint gap. Hence, careful consideration of the synergistic effects of the laser process parameters, joint configuration and set-up conditions (e.g. filler wire angle relative to workpiece and laser beam) must be performed to obtain an operating window for manufacturing that yields integral welds of high quality and performance. In this work, the gap tolerance of Ti–6Al–4V, an alpha–beta (α–β) alloy, was studied with this intent.

Experimental procedure

As received mill annealed grade 5 Ti–6Al–4V sheets (AMS 4911) with a thickness of 3·2 and 5·1 mm were sectioned into coupons with dimensions of approximately 75 mm in length × 38 mm in width. The faying and adjacent surfaces of each specimen were brushed and then cleaned with ethanol to remove surface oxides and any contaminants prior to clamping and welding. The welding equipment consisted of a 4 kW continuous wave solid state Nd:YAG laser system equipped with an ABB robot and a magnetic holding fixture. A collimation lens of 200 mm, a focal lens of 150 mm and a fibre diameter of 0·6 mm were utilised to produce a focusing spot diameter of approximately 0·45 mm. Owing to the high reactivity of titanium with atmospheric elements, especially in the liquid state and at high temperatures, adequate measures were taken to shield the fusion zone (FZ) and the heated surfaces until these regions were cooled below 350°C. High purity argon at a flowrate of 23·6 L min^{-1} (50 cfh) was used to shield the top surface of the workpiece. The shielding of the root and the trailing gas shield on the top surface were performed using helium at a total flowrate of 66·1 L min^{-1} (140 cfh). The laser beam was focused at the top surface of the workpiece. The effect of joint gap was investigated at a welding speed of 1·69 m min^{-1} and a laser power of 3·0 kW for the 3·2 mm thick sheet and a welding speed of 3·0 m min^{-1} and a laser power of 4·0 kW for 5·1 mm thick sheet. These optimum parameters were used based on the results of a systematic investigation in an earlier work.[10] Ti–6Al–4V filler wire (AMS 4956A ELI), with a nominal diameter of 1·14 mm, was fed at a fixed angle of a 30° relative to the top surface of the workpiece. It has been reported that the angle at which the filler wire is normally fed lies between 10 and 60° with the workpiece surface, where a smaller angle causes the wire to intersect with a large area of the laser beam resulting in high reflection in laser beam and vaporisation of the wire.[11] Hence, in this work, an intermediate angle of 30° was selected. The filler wire feedrate was calculated from a volume flowrate constancy equation

$$\text{Wire feedrate} = \frac{\text{Welding speed} \times \text{Gap area}}{\text{Filler wire area}} \quad (1)$$

For a given joint gap, the wire feedrate was calculated using equation (1). Table 1 lists the main processing parameters used in this study. Three transverse sections were cut from each joint and mounted using cold setting epoxy resin. The samples were ground with 1200/4000 grit SiC paper and then polished with 0·05 μm colloidal silica suspension (Struers OP-S) to produce a mirror-like finish. Kroll's reagent (1–3 mL HF + 2–6 mL HNO_3 + 100 mL H_2O) was used for 6–10 s, depending on the zones of interest. Microstructural examination was carried out using an inverted optical microscope (Olympus GX710) equipped with an Olympus digital camera XC50 and AnalySIS Five image analysis software for measurement of the joint geometry. The Vickers microindentation hardness was measured using a Struers Duramin A-300 hardness tester at a load of 500 g, a dwell period of 15 s and an interval of 0·2 mm.

Results and discussion

Weld geometry

Figure 1 gives an overview of the transverse sections of the laser welds for various joint gaps for both the 3·2 and 5·1 mm thick Ti–6Al–4V. All the joints were fully penetrated up to a gap width of 0·6 mm, but a lack of penetration defect appeared at a joint gap of 0·7 mm.

Figure 2 shows the effect of joint gap on the weld geometry for the two sheet thicknesses. The area of the FZ and HAZ, as well as the width of the FZ at the top, middle and root were relatively similar up to a joint gap width of 0·6 mm. This is contradictory to the results reported by Cao *et al.*[12] in which the FZ and HAZ dimensions usually decreased to some extent with increasing joint gap width for laser welded 3 mm Ti–6Al–4V sheets at a power of 4 kW. Their finding was reasoned on the basis of laser energy losses through

the joint gap, i.e. with increasing gap width the effective energy for welding decreases and results in a smaller FZ and HAZ. In the present study, optimised laser process parameters were used and welding was performed at low laser power densities to minimise evaporative losses from the molten metal. To this end, the laser beam energy effectively generates a molten weld pool that rapidly fills the joint gap and minimises energy losses through the gap width. Hence, for the case of optimised process parameters, the low or relatively constant energy loss through the joint gap diminishes the influence of the gap width on the FZ and HAZ geometry. It is noteworthy that the maximum joint gap that can be bridged (0·6 mm) was slightly larger than the beam size (approximately 0·5 mm). However, if the joint gap is much larger than the spot size, the large gap width cannot be effectively bridged, as demonstrated at a gap width of 0·7 mm. In this case, more laser energy loss occurs through the large gap width, which can decrease the amount of molten weld pool and lead to the formation of a lack of penetration defect at the large joint gap.

Microstructure

Figure 3 shows the typical microstructures of the base metal for the two sheet thicknesses in the as received (mill annealed) condition. The base metal microstructure of the 3·2 mm thick sheet consisted of equiaxed α grains with intergranular β, while the 5·1 mm thick sheet consisted of equiaxed primary α grains and equiaxed transformed β grains with a lamellar $\alpha+\beta$ structure. For the two sheet thickness welded in the present study, the macro- and microstructural constituents of the FZ and HAZ were also examined by optical microscopy. As apparent in Fig. 1, the FZ macrostructure of the Ti–6Al–4V laser welds consisted of columnar prior beta grains that originated during solidification from the molten weld pool. The beta grains that nucleated at the fusion boundary solidified towards and impinged at the weld centreline. Figure 4 shows that the microstructural characteristics within the prior beta grains of the FZ for the 3·2 and 5·1 mm thick sheets consisted mainly of martensite (α') with small amount of retained β (not visible under optical microscope). This formation of α' is expected under the rapid solidification conditions typical of laser welding. The HAZ microstructure consisted of a mixture of the microstructural constituents in the FZ and base metal, as shown in Fig. 5. Specifically, the HAZ microstructure consisted almost entirely of the transformed β grains having a martensitic structure near the FZ boundary. This region is termed near HAZ. With increasing distance from the FZ boundary (i.e. in the far HAZ), the fraction of α' in the microstructure decreased and increasing remnants of the base metal constituents were observed, namely α grains with intergranular β for the 3·2 mm thick sheet (Fig. 5*a*) or equiaxed primary α and equiaxed transformed β grains having a lamellar $\alpha+\beta$ structure for the 5·1 mm thick sheet (Fig. 5*b*). It is noteworthy that no significant differences were observed for the FZ microstructure over the joint gap widths investigated in this study for the two sheet thicknesses, mainly due to the matching of the filler wire composition with the base metal and relatively constant heat input.

Defects

Underfill and porosity were the two main defects observed as revealed in the transverse sections of the laser welds (Fig. 1). Loss of material from the top surface due to evaporation, expulsion, spatter and flow of the molten material is most likely the main reason for the formation of the underfill defect during laser welding of Ti–6Al–4V.[13] Specifically, a high laser power (i.e. high power density) has been reported to result in underfill defects through material evaporation in Ti–6Al–4V welds.[14] In addition, metal flow can also cause the formation of the underfill, particularly at high welding speeds.[13] For titanium alloys, the reduced surface tension at high temperature may negatively affect the adhesion of the liquid metal to the solid material, possibly aiding in the formation of the underfill defect. The presence of underfill defects reduces the cross-sectional thickness of the weld, which leads to local stress concentration and 'premature' crack formation that reduce the tensile and fatigue strength of the welds. The effect of joint gap width on the relative area and depth of the underfill defects, as shown in Fig. 6,

Table 1 Process parameters

Thickness/mm	Joint gap/mm	Laser power/kW	Defocusing distance/mm	Laser beam size/mm	Welding speed/m min^{-1}	Wire feedrate/m min^{-1}
3·2	0·0	3	−1	0·49	1·69	0·00
	0·1					0·53
	0·2					1·05
	0·3					1·58
	0·4					2·10
	0·5					2·63
	0·6					3·16
5·1	0·0	4	−1	0·49	1·00	0·00
	0·1					0·50
	0·2					1·00
	0·3					1·50
	0·4					2·00
	0·5					2·50
	0·6					3·00

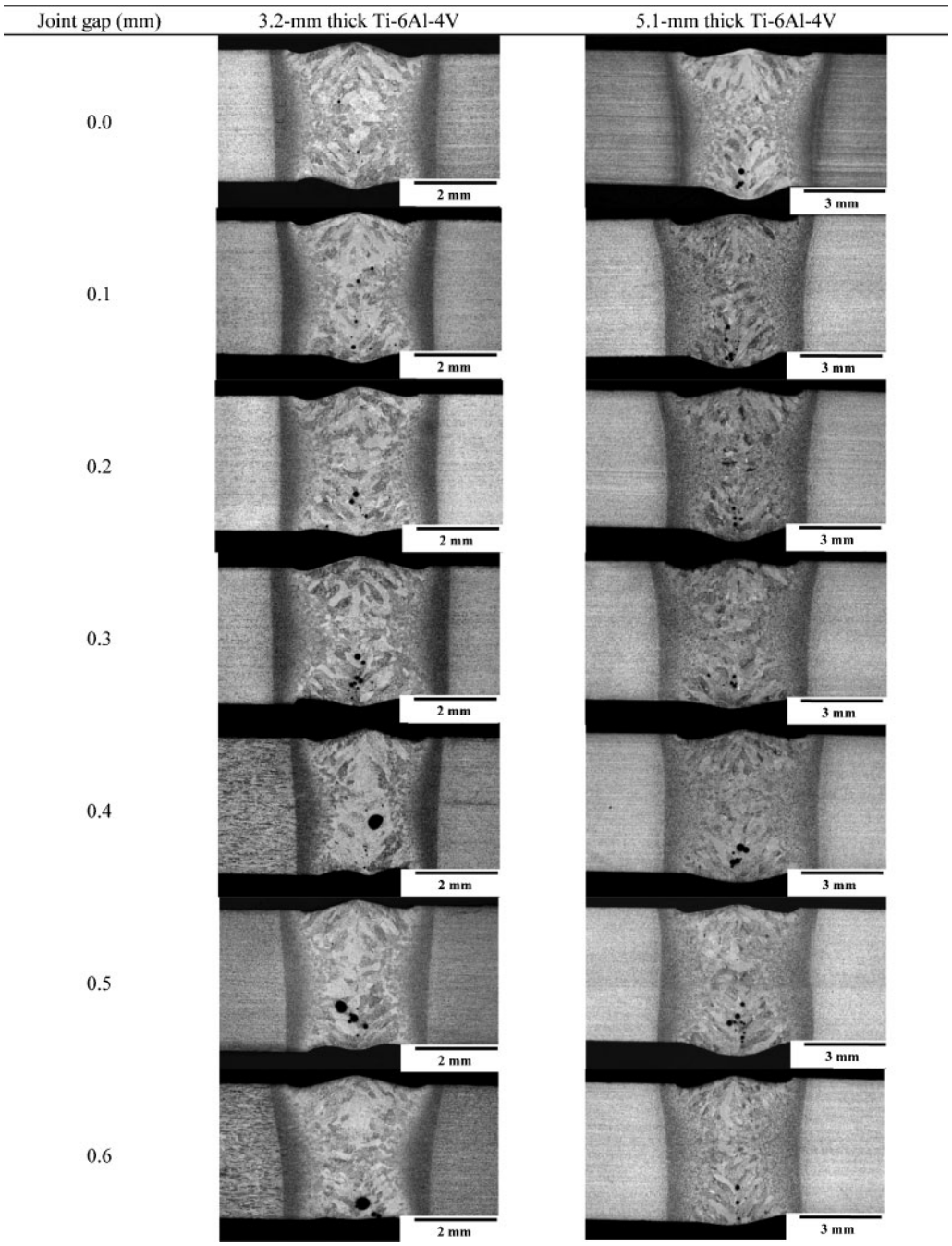

1 Effect of joint gap width on transverse section geometry for two sheet thicknesses

appears to be almost negligible, with perhaps the exception of the 5·1 mm thick weld obtained at a joint gap of 0·6 mm. As discussed above, the optimised laser process parameters applied in the present study effectively reduced the evaporative material losses and imparted the beam energy efficiently to form the molten weld pool. Thus the relatively constant underfill dimensions are mainly due to metal flow in this study, with the exception of the low underfill value at a joint gap of 0·6 mm that is probably due to the instigation of some energy loss as the gap width surpasses the laser beam diameter. It was reported that the use of filler wire can reduce the underfill defect.[12] This is true when the evaporative loss becomes serious at relatively high power density. At a low evaporative loss, as demonstrated in this study using optimum processing parameters, the use of the filler wire does not lead to the improvement in the underfill defect. It is noteworthy that according to the AWS D17-1,[15] the maximum underfill depth allowable in a weld is 7% of the sheet thickness, or 0·22 and 0·36 mm for the 3·2 and 5·1 mm thick sheets respectively. As the measured maximum underfill depths were 0·15 and 0·36 mm for the 3·2 and 5·1 mm thick welded samples (i.e. 5% and 7% of the

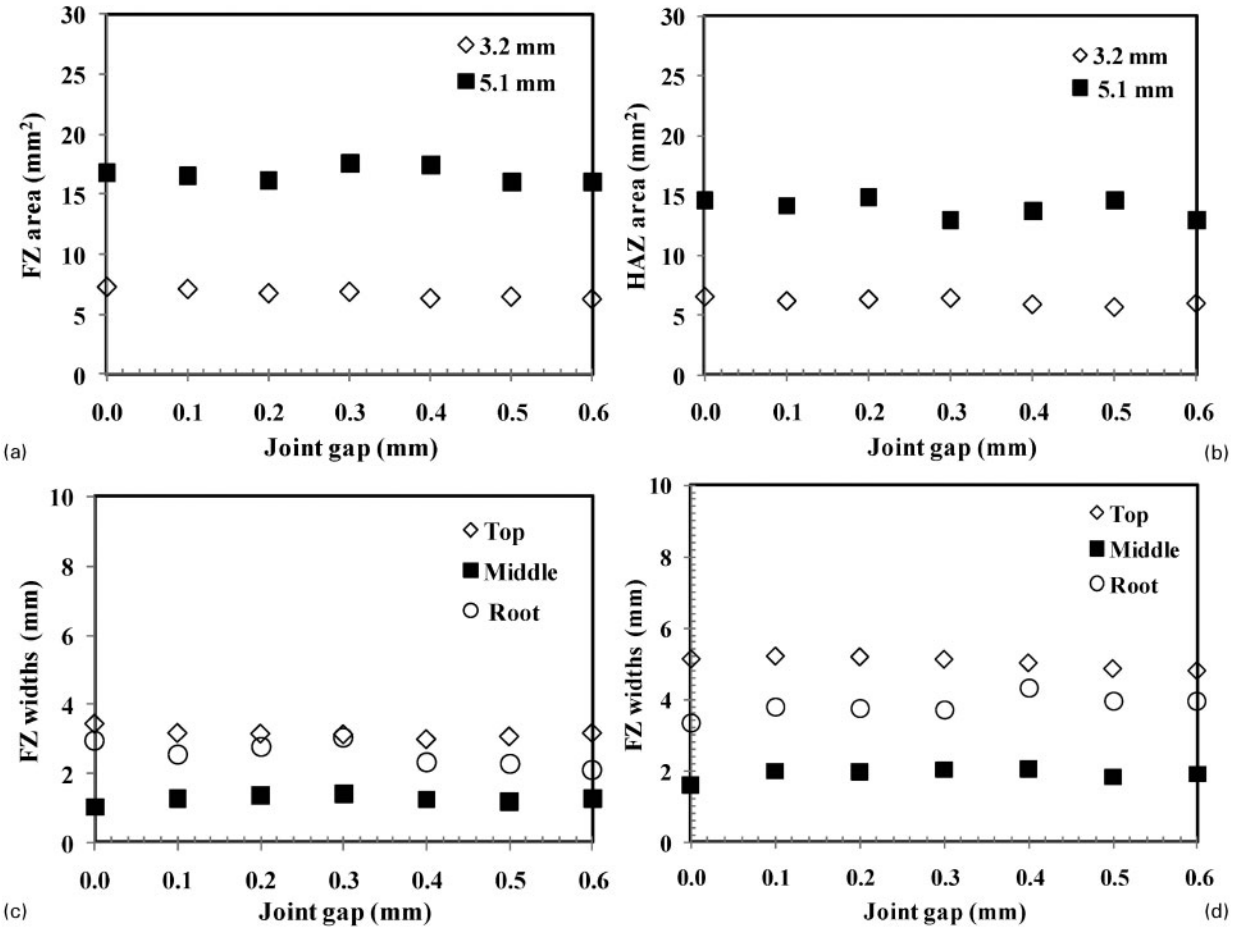

a 3·2 and 5·1 mm thick Ti–6Al–4V; *b* 3·2 and 5·1 mm thick Ti–6Al–4V; *c* 3·2 mm thick Ti–6Al–4V; *d* 5·1 mm thick Ti–6Al–4V

2 Effect of joint gap width on FZ and HAZ dimensions for two sheet thicknesses

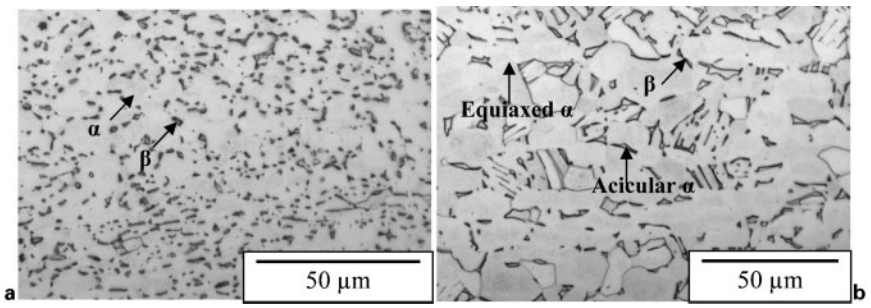

a 3·2 mm thick Ti–6Al–4V; *b* 5·1 mm thick Ti–6Al–4V

3 Typical base metal microstructures

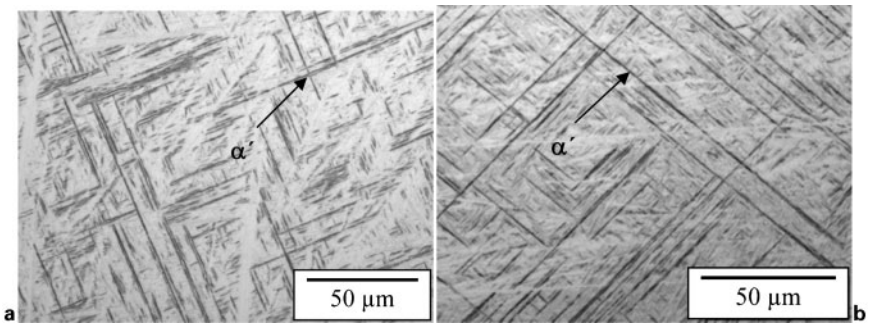

a 3·2 mm thick Ti–6Al–4V; *b* 5·1 mm thick Ti–6Al–4V

4 Typical microstructures for FZ at joint gap width of 0·4 mm

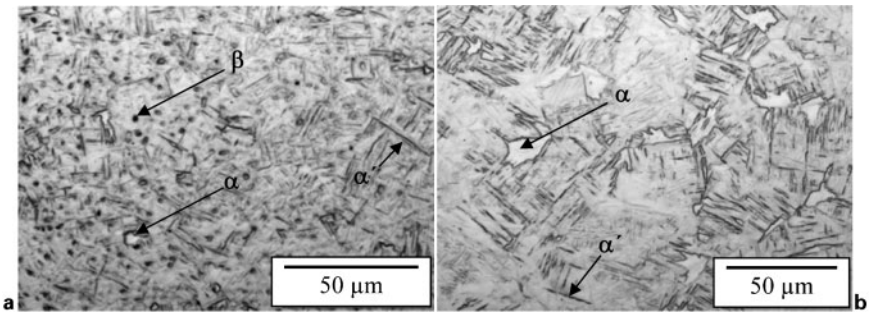

a 3·2 mm thick Ti–6Al–4V; *b* 5·1 mm thick Ti–6Al–4V

5 Typical microstructures for the far-HAZ at a joint gap width of 0·4 mm

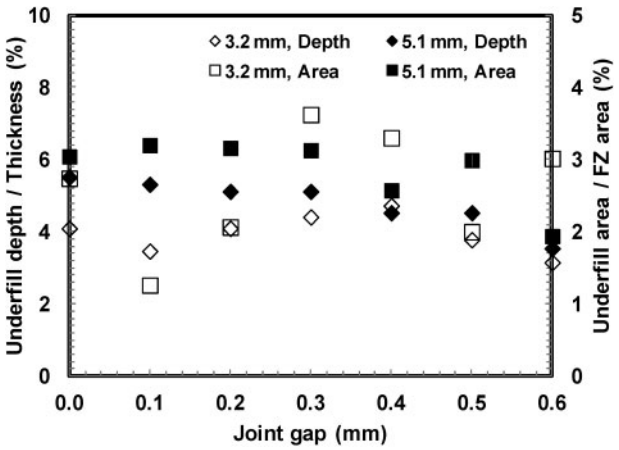

6 Effect of joint gap on underfill defects

sheet thickness) respectively, the Ti–6Al–4V laser welds manufactured in this work met the AWS D17-1 standard requirements.

Porosity formation in the laser welding of Ti–6Al–V is another main concern. The porosity is mainly caused by the gas bubbles that are entrapped in the molten materials during welding that cannot escape before solidification.[1] The formation of gas porosity is probably due to the contamination from grease, oil and dirt existing on the surfaces of the workpieces and filler materials. For titanium joints, hydrogen is considered to be the primary gas source for the presence of gas porosity.[16] However, keyhole collapse[17] may also contribute to porosity formation. In particular, keyhole stability is related to the welding speed and the balance in forces acting in the keyhole (mainly vapour pressure and surface tension).[18] It is noteworthy that the pores caused by unstable keyholes are usually located in the lower half of the weld.[19] In general, the main concern related to the presence of porosity is a reduction in the weld cross-sectional area, especially when there are a large number of small pores concentrated in one region that can coalesce into large pores.[11]

The typical pores apparent in the FZ for different joint gap widths, as shown in Fig. 7, are predominantly spherical in shape, indicating that these are most likely gas porosity. Also some of the pores were located towards the root of the FZ, suggesting that the keyhole instability is another reason for porosity formation. Figure 8 shows the relationship between the joint gap width and total porosity area. The porosity area and percent porosity area to the FZ area tend to increase with increasing joint gap width. This can be reasoned by considering that the quantity of filler wire addition increases with increasing gap width and can be a source for porosity formation (i.e. contamination of the filler

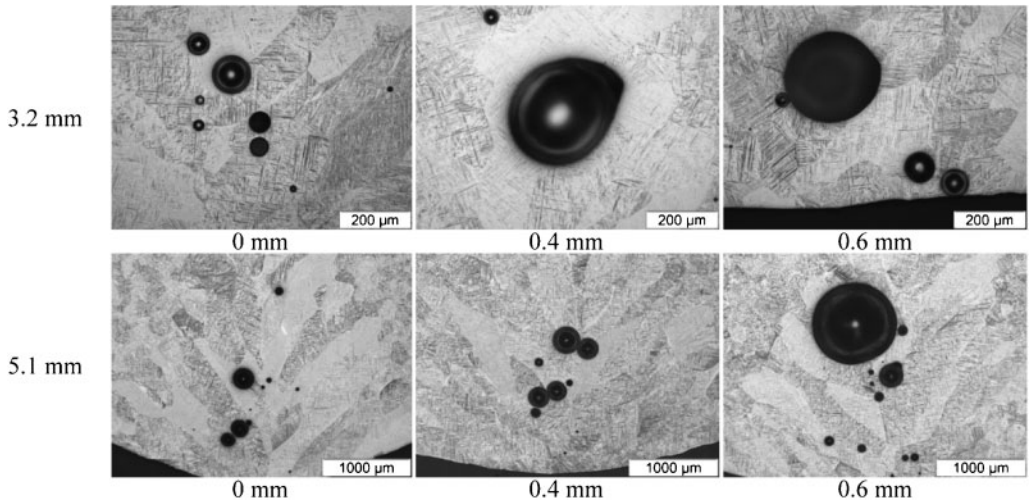

7 Typical pores observed at various joint gap widths for two sheet thicknesses

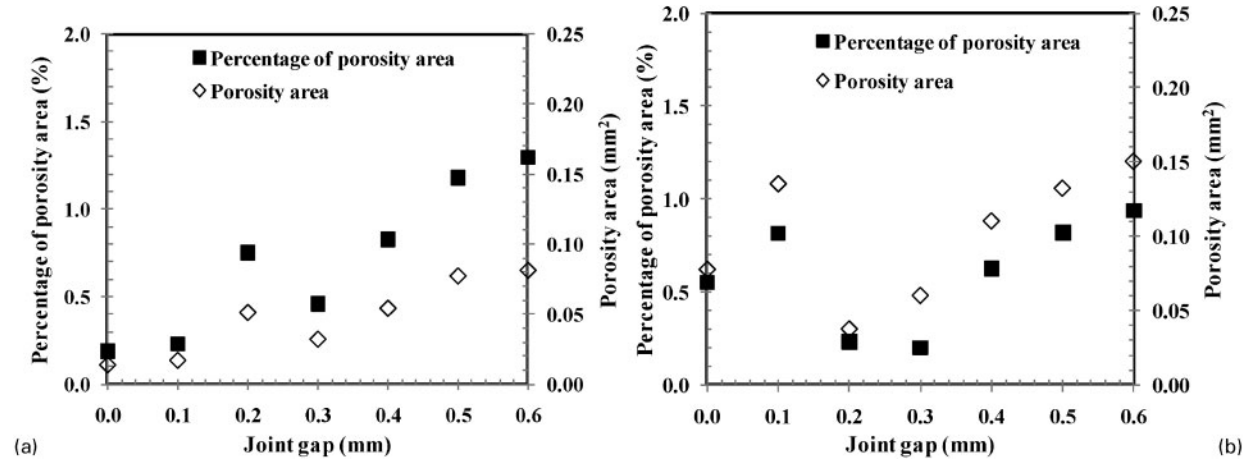

a 3·2 mm Ti–6Al–4V; *b* 5·1 mm Ti–6Al–4V

8 Effect of joint gap width on porosity area and area percentage

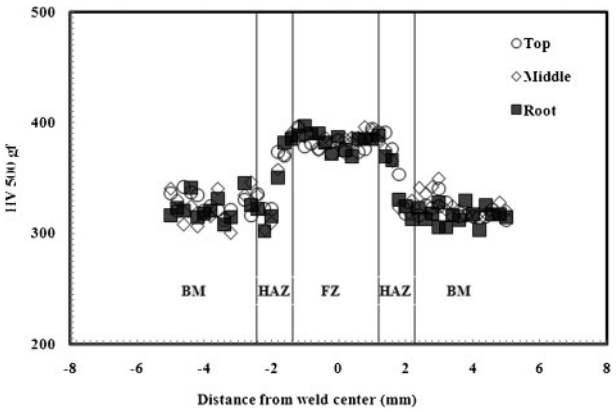

9 Typical microindentation hardness profile at joint gap width of 0·4 mm for the 3·2 mm thick laser welded Ti–6Al–4V

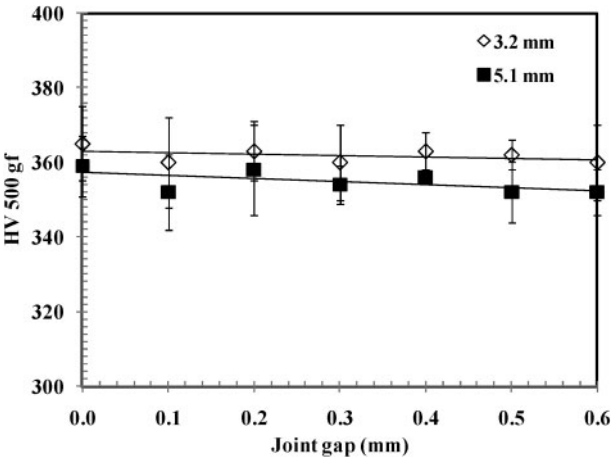

10 Effect of joint gap width on FZ average hardness

wire surface). Though the maximum percentage of porosity area remained low (1·3%) up to a gap width of 0·6 mm, the effect of the pores on the mechanical strength and ductility must be considered as the coalescence of small closely spaced pores can cause premature failure.

Microindentation hardness

The typical hardness profile for the laser welded Ti–6Al–4V sheets, as shown in Fig. 9, exhibited a hardness maximum in the FZ and the near HAZ, and, just beyond the near HAZ, a decrease in hardness in the far HAZ until reaching the base metal hardness value. The occurrence of a maximum hardness in the FZ and near HAZ is related to the martensitic microstructure. With increasing distance from the FZ boundary, the hardness values in the far HAZ decrease because the fraction of α' in the microstructure decreases. The average FZ hardness was approximately 361 ± 4 HV for the 3·2 mm thick welds and 354 ± 5 HV for the 5·1 mm thick weld, indicating a 15·7% and 13·5% increase in the FZ hardness as compared to the base metal. A slightly higher FZ hardness for the 3·2 mm thick welds was observed, inevitably due to the higher cooling rate that transpires in the thinner section, as compared to the 5·2 mm thick welds. The effect of joint gap width on the average hardness of the FZ is shown in Fig. 10. The average FZ hardness tends to remain relatively constant over the range of joint gap widths examined in this work. The dashed line on the graph indicates the average base metal hardness value of 312 HV.

Conclusions

Ti–6Al–4V sheets, 3·2 and 5·1 mm in thickness, were welded using a continuous wave Nd:YAG laser system with the addition of Ti–6Al–4V filler wire to investigate the effect of joint gap on the weld quality. The main results can be summarised as follows:

1. Full weld penetration was obtained up to a joint gap width of 0·6 mm, slightly larger than the beam size (approximately 0·5 mm) used.

2. Increasing joint gap width had a negligible effect on the FZ and HAZ geometries under the optimum laser process parameters applied in this study.
3. The main defects observed were porosity and underfill, but these remained within the aerospace welding specifications. No cracks were observed in the weldments.
4. The FZ microstructure consisted mainly of martensite.
5. The HAZ microstructure consisted almost entirely of martensite near the FZ boundary and with increasing distance from the FZ boundary, the fraction of martensite in the microstructure decreased until the base metal microstructure was attained.
6. No significant variation in the FZ hardness was observed with increasing joint gap width.
7. The FZ hardness was roughly 13–16% higher than that of the base metal.

Acknowledgements

The authors would like to thank E. Poirier and X. Pelletier for their technical support during the laser welding experiments and metallographic sample preparation.

References

1. E. Akman, A. Demir, T. Canel and T. Sinmazçelik: 'Laser welding of Ti6Al4V titanium alloys', *J. Mater. Process. Technol.*, 2009, **209**, (8), 3705–3713.
2. A. B. Short: 'Gas tungsten arc welding of $\alpha+\beta$ titanium alloys: a review', *Mater. Sci. Technol.*, 2009, **25**, 309–324.
3. Q. Yunlian, D. Ju, H. Quan and Z. Liying: 'Electron beam welding, laser beam welding and gas tungsten arc welding of titanium sheet', *Mater. Sci. Eng. A*, 2000, **A280**, (1), 177–181.
4. F. Caiazzo, F. Curcio, G. Daurelio and F. Memola Capece Minutolo: 'Ti6Al4V sheets lap and butt joints carried out by CO_2 laser: mechanical and morphological characterization', *J. Mater. Process. Technol.*, 2004, **149**, (1–3), 546–552.
5. J. C. Ion: 'Laser processing of engineering materials; principles, procedure and industrial application'; 2005, Oxfrod, Elsevier Butterworth-Heinemann.
6. U. Dilthey, D. Fuest and W. Scheller: 'Laser welding with filler wire', *Opt. Quantum Electron.*, 1995, **27**, (12), 1181–1191.
7. X. Cao, M. Jahazi, J. P. Immarigeon and W. Wallace: 'A review of laser welding techniques for magnesium alloys', *J. Mater. Process. Technol.*, 2006, **171**, (2), 188–204.
8. M. J. Donachie: 'Titanium: a technical guide'; 1989, Materials Park, OH, ASM International.
9. ASM International: 'ASM handbook', Vol. 6, 'Welding, brazing, and soldering'; 1993, Materials Park, OH, ASM International.
10. A. S. H. Kabir: 'Nd:YAG laser welding of Ti–6Al–4V alloy', MSc thesis, Concordia University, Montreal, Que., Canada, 2011.
11. C. Dawes: 'Laser welding'; 1992, New York, McGraw-Hill, Inc.
12. X. Cao, G. Debaecker, E. Poirier, S. Marya, J. Cuddy, A. Birur and P. Wanjara: 'Tolerances of joint gaps in Nd:YAG laser welded Ti–6Al–4V alloy with the addition of filler wire', *J. Laser Appl.*, 2011, **23**(1), 012004(1–10).
13. M. Pastor, H. Zhao, R. P. Martukanitz and T. DebRoy: 'Porosity, underfill and magnesium loss during continuous wave Nd:YAG laser welding of thin plates of aluminum alloys 5182 and 5754', *Weld. J.*, 1999, **78**, 207s–216s.
14. X. Cao and M. Jahazi: 'Effect of welding speed on butt joint quality of Ti–6Al–4V alloy welded using a high-power Nd:YAG laser', *Opt. Lasers Eng.*, 2009, **47**, (11), 1231–1241.
15. AWS: 'Specification for fusion welding for aerospace application', AWS D17·1, American Welding Society, Miami, FL, USA, 2001.
16. Z. Khaled: 'An investigation of pore cracking in titanium welds', *J. Mater. Eng. Perform.*, 1994, **3**, (3), 419–434.
17. L. Tsay, Y. P. Shan, Y. H. Chao and W. Shu: 'The influence of porosity on the fatigue crack growth behavior of Ti–6Al–4V laser welds', *J. Mater. Sci.*, 2006, **41**, (22), 7498–7505.
18. W. W. Duley: 'Laser welding'; 1998, New York, Wiley-Interscience.
19. X. Cao, W. Wallace, C. Poon and J. P. Immarigeon: 'Research in laser welding of wrought aluminum alloys. II. Metallurgical microstructures, defects, and mechanical properties', *Mater. Manuf. Processes*, 2003, **18**, (1), 23–49.